Journal of Cancer Therapy, **2009, 1, 52-58**
Published Online September 2009 in SciRes (www.SciRP.org/journal/cancer)

The Experimental Study of a Precision Parallel Manipulator with Binary Actuation: With Application to MRI Cancer Treatment

ABSTRACT

In this paper the performance of a high-precision parallelrobot manipulator with bistable actuation is experimentally evaluated. The manipulator is for performing prostate cancer biopsy and treatment within the bore of a Magnetic Resonance Imaging (MRI) system. The analysis and simulations have shown that this bistable manipulator is able to perform well with dielectric elastomer actuators that have been shown to be compatible with the high magnetic fields of an MRI. In this work an experimental prototype system was developed and tested. The results show that it provides the precise needle placement required by the medical task.

***Keywords*:** *call for implementation*, *software development*, *open community*, *integration*

1. Introduction

In this paper the performance of a high-precision parallel robot manipulator with bistable actuation for cancer treatment inside the bore of an MRI (Magnetic Resonance Imaging) system is experimentally evaluated. A laboratory prototype of this system is shown in Figure 1.

Current robotic actuation technology is not adequate for many applications. It is heavy, complex, expensive, and requires complex electronics. Binary robotic systems have been proposed to overcome the limitations of conventional actuation [1]. Applications considered include space exploration systems and medical devices [2,3]. A binary system is driven by actuators that switch between two possible stable states. These systems are simple, do not use power to hold their state, and require fewer sensors than traditional systems [4]. However, the lack of practical binary actuators has been a major limitation in the past.

Recent advances have made Dielectric Elastomer Actuators (DEAs) an effective and practical solution to this problem [5,6]. They are lightweight, simple and inexpensive and virtually all plastic.

It has been shown that using DEAs in a bistable manner, intermittently at high speeds, avoids the reliability problems that have plagued them in their use in conventional systems. Furthermore, unlike conventional actuators they have been shown to be compatible with MRI systems. DEAs operate normally within MRIs and do not affect the MRI's image quality [7].

Figure 2 shows a bistable actuator using an antagonistic pair of DEAs to switch a bistable element between its two stable positions [6]. A parallel structure improves the stiffness of a robotic system [8].

However, unlike conventional robotic systems that use one high precision continuous actuator per DOF to achieve good accuracy, parallel bistable systems require many actuators per DOF to obtain high precision. This results in an over constrained system. Compliance can be used to accommodate for these extra constraints using "Elastic Averaging" where the compliance of the system mediates between the bistable actuators to achieve high precision positioning [9]. Hence, elastically averaged parallel binary robotic systems based on MRI compatible DEAs have been considered for in-bore Magnetic Resonance Imaging (MRI) cancer therapy manipulators [3].

2. Application: An MRI Cancer Therapy Manipulator

The objective of this work is to show experimentally that such a system can achieve the medically mandated precision. Being able to perform cancer therapy in the bore of an MRI, using a manipulator, where a tumor can be observed by a surgeon outside the MRI, can greatly improve cancer survival rates and quality of life after treatment. For example, using a real-time image and an MRI compatible manipulator would allow a surgeon to accurately guide a biopsy needle (which is visible in the MRI image) to determine if a tumor (also visible) is malignant while avoiding vital structures. However, the magnetic fields of MRIs limit the use of conventional manipulators

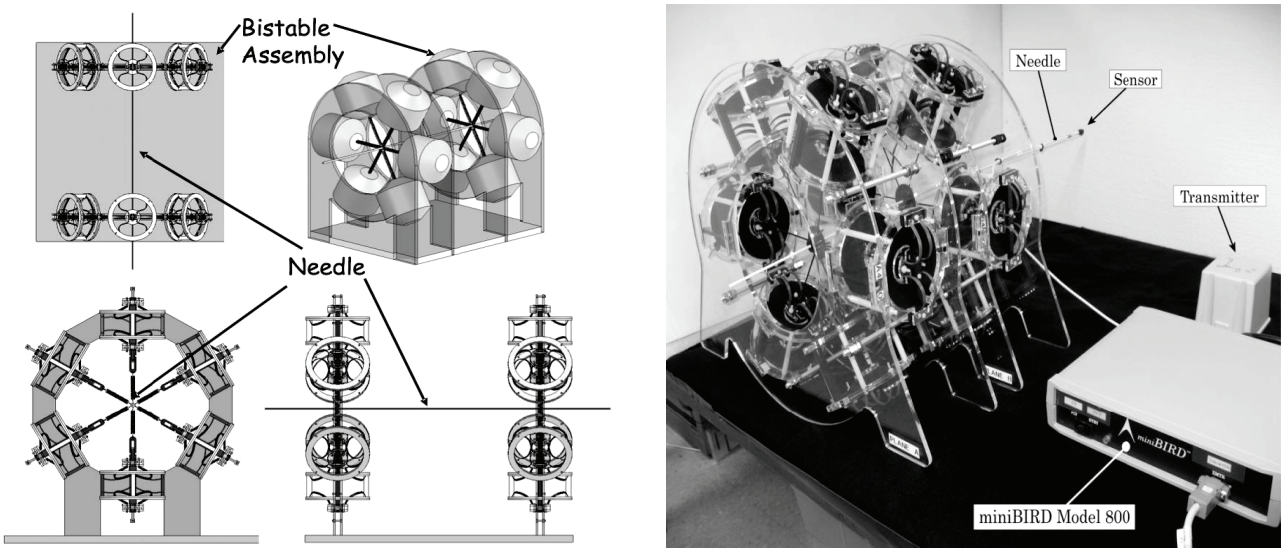

a. System Concept **b. Experimental System**

Figure 1. A Laboratory Prototype MRI Man

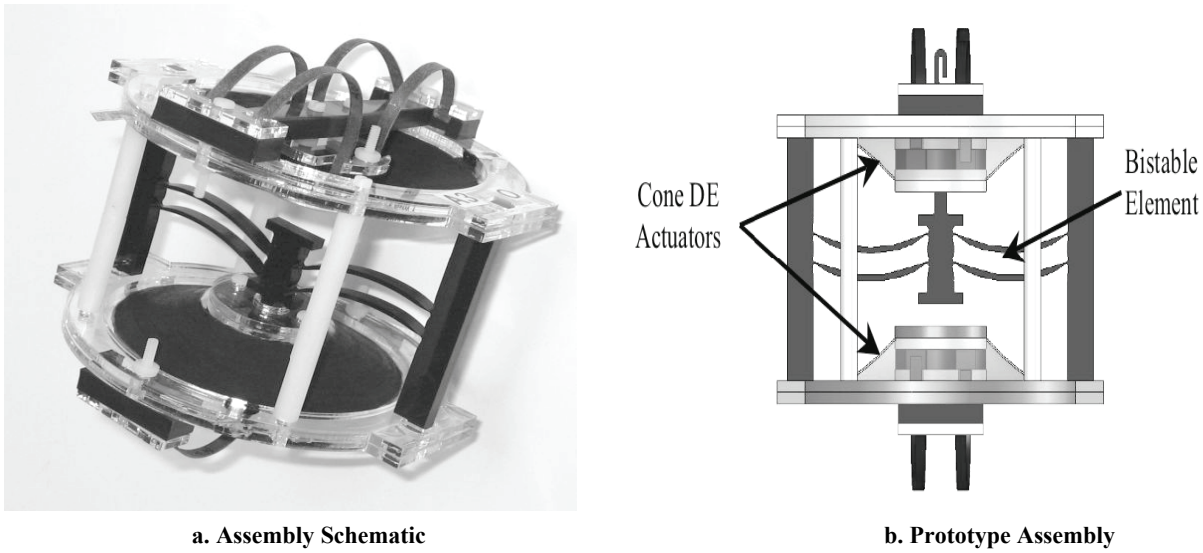

a. Assembly Schematic **b. Prototype Assembly**

Figure 2. A bistable actuator assembly using antagonistic DEAs

within the bore of the MRIs. To date only limited success has been achieved in designing effective and reasonably priced systems [10,11]. Hence MIT has been exploring, with researchers from Harvard University's Brigham and Women's Hospital, parallel MRI manipulator designs using bistable DEAs focusing on prostate cancer detection and treatment [12,13].

Prostate cancer is the most common cancer in men and the number two cause of cancer deaths in men [14]. Transperineal needle biopsy provides the most conclusive diagnosis of prostate cancer. In this method a needle is inserted into the prostate and a small piece of tissue is removed. After detected, a malignant tumor can be treated by inserting a transperineal brachytherapy needle through the perineum to introduce tiny radioactive pellets, or a cryogenic fluid into the tumor (see Figure 3) [15]. These are outpatient procedures with high success rates and low risk of side effects, compared to such procedures as radical prostatectomy, hormone therapy and transrectal brachytherapy. However, they require precise needle placement. Currently, ultrasound imaging is used for needle placement. In-bore MR scans would provide much more detailed and effective images, motivating this research to design a DEA manipulator for transperineal needle insertion that can operate in the bore of an MRI while being visually guided in real time by a surgeon.

3. Manipulator Design

The requirements for the device have been developed by researchers at Brigham and Women's Hospital. A more detailed description of these requirements and the design can be found in references [13,16]. The device must fit

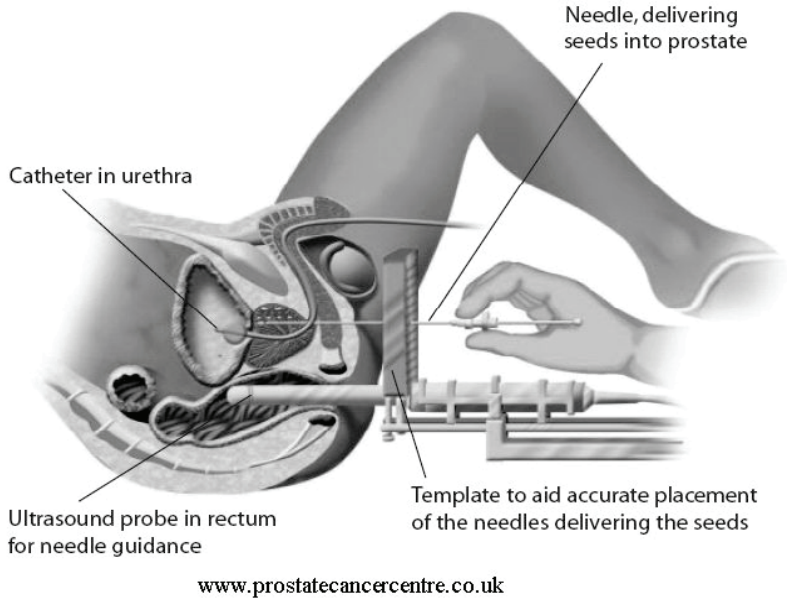

Figure 3: Transperineal brachytherapy procedure

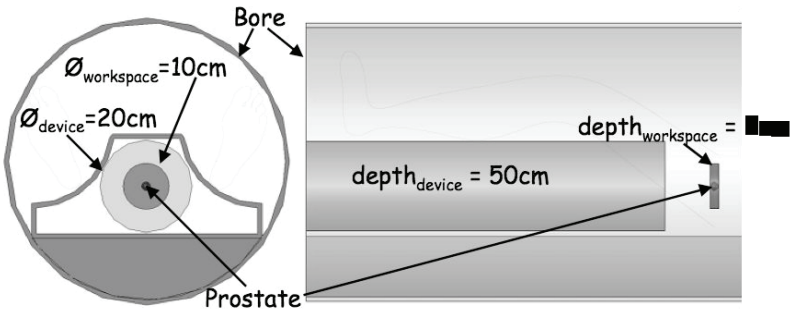

Figure 4: Manipulator size constraints

between the patient's legs while inside the bore of the MRI (see Figure 4). This requires it to be smaller than a 20cm diameter cylinder approximately 50cm in length.

The manipulator must be able to reach a tumor in the prostate by penetrating the perineum approximately 10 cm with an accuracy of ±5mm. This accuracy is necessary to be able to detect and destroy tumors in the early stage of development. The required workspace is roughly a 10cm diameter cylinder, 2cm deep. This is selected to accommodate the enlarged prostates of cancer patients. The maximum needle penetration force specification of 14N and maximum force perpendicular the needle of 1.6N were set based on animal muscle tissue tests and values in the published literature [16]. Figures 1 and 5 show the manipulator's kinematic configuration. It is a parallel manipulator that has two planes with six-bistable actuator elements symmetrically distributed around the center. Each actuator can be independently activated to a predetermined extension. The surgical needle runs through a tube at the nominal center of each actuator plane and advances from Plane 1 through Plane 2 to the target. Each bistable actuator assembly is attached to the center of the plane by springs with different spring constants. The bistable assembly is composed of two antagonistic cone-shaped actuators that switch a bistable device to one of two positions (see Figure 2). Figure 5 shows all bistable assemblies in the "off" position. When switched to the "on" position, the bistable devices will move radially by a fixed amount.

4. Manipulator Analytical Model

Each plane of the system has a set of nodes that are the inputs. The nodes' motions are the binary actuator extensions between two known positions. A binary system can only reach a finite set of discrete points. To obtain a fine output resolution and to meet the system specification of +/- 5mm, the manipulator must have many degrees-offreedom. The binary actuation, Q , of the modules are:

$$Q = [a_1 ,a_2 ,...,a_i ,...,a_n] \quad (1)$$

where n is number of the actuators in the plane, and a_i (i 1,2,..., n)= 1 or 0, the values of 1 or 0 for ON or OFF state of the ith binary actuator.

The deformation of the springs and their forces due to

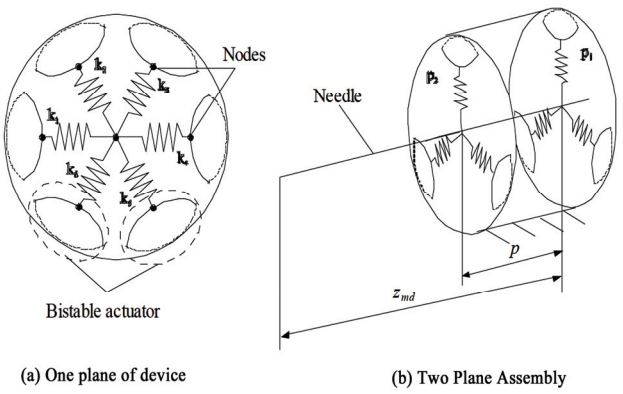

Figure 5. Schematic of proposed manipulator

the external forces at the center point and the motion of nodes 1 to *n* of the bistable assemblies are shown in Figure 6. In the *O-xy* coordinate system shown in Figure 6, a closed-loop position constraint equation is written as:

$$\mathbf{l}_i = \mathbf{l}_{s\,i} - \mathbf{U} \tag{2}$$

where $\mathbf{l}_i$ is the position vector of the *i*th spring between the two connection points to the center point and the *i*th actuator, $\mathbf{I}_i = O'A_I = l_i\mathbf{V}_i$, $\mathbf{V}_i$ is the unit vector of $\mathbf{I}_i$, $\mathbf{V}_i = \{\cos\varphi_i, \sin\varphi_i\}^T$,and φ_i is the unit vector and orientation angle of $\mathbf{I}_i$; $\mathbf{U}$ is the vector displacement of center point, $\mathbf{U} = OO' = U\mathbf{e}'$; $\mathbf{e}'$ is the unit vector of $\mathbf{U}$, $\mathbf{e}' = \{\cos\phi, \sin\phi\}^T$, ϕ is the orientation angle of $\mathbf{U}$; and $\mathbf{I}_{si}$ is the displacement vector of the *i*th spring between the two connection points to the center point and the *i*th actuator before all actuators turn off. $\mathbf{I}_{si} = OA_i = (l_{oi} + \delta_i)\mathbf{W}_i$. δ_i is the stretched length of the *i*th spring along axis of *i*th undeformed spring.

$$\delta_i = \Delta_i + a_i\xi_i \tag{3}$$

in which Δ_i is the pre-stretching length of the *i*th spring along axis of *i*th undeformed spring, and ξ_i is the stroke of *i*th actuator along axis of *i*th undeformed spring. The variable l_{oi} is the undeformed length of the *i*th spring. $\mathbf{W}_i$ is the unit vector of the *i*th spring along the *i*th undeformed spring. The vector $\mathbf{W}_i = \{\cos\theta_i, \sin\theta_i\}^T$, θ_i is the position angle of the *i*th undeformed spring.

Then one can write:

$$l_i\mathbf{V}_i = (l_{oi} + \Delta_i + a_i\xi_i)\mathbf{W}_i - U\mathbf{e}' \tag{4}$$

The deformation of the *i*th spring along the axis of the *i*th deformed spring is

$$\begin{aligned}\delta_i\mathbf{V}_i = (l_i - l_{oi})\mathbf{V}_i = (l_{oi} + \Delta_i + a_i\xi_i)\mathbf{W}_i \\ - U\mathbf{e}' - l_{oi}\mathbf{V}_i, i = 1,2,...,n\end{aligned} \tag{5}$$

and the internal force of the *i*th actuator is:

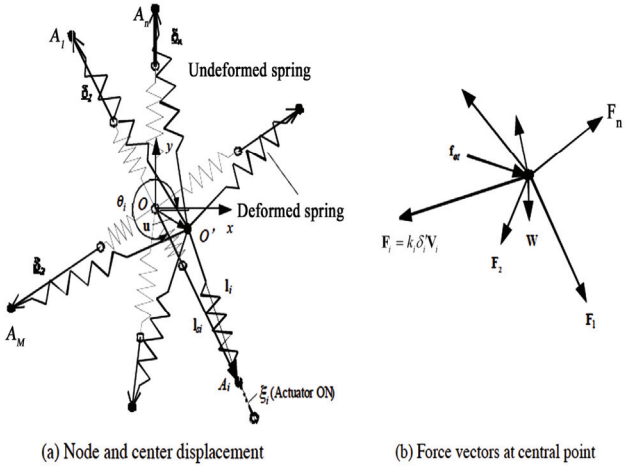

Figure 6. Actuation center point rree-body diagrams

$$\begin{aligned}\mathbf{F}_i = -k_i\delta_i'\mathbf{V}_i = -k_i[(l_{oi} + \Delta_i + a_i\xi_i)\mathbf{W}_i \\ - U\mathbf{e}' - l_{oi}\mathbf{V}_i], i = 1,2,...,n.\end{aligned} \tag{6}$$

where k_i is the stiffness of the *i*th spring.

Static equilibrium in the plane requires that the sum of the forces at the center point to be zero:

$$\sum\mathbf{F} = \sum_i \mathbf{F}_i + \mathbf{f}_{ext} + \mathbf{W} = \mathbf{0} \tag{7}$$

where $\mathbf{f}_{ext}$ and $\mathbf{W}$ are the external force vector and weight vector at center point, respectively.

The workspace of each plane of the system can be obtained by solving Eqs. (5) and (6), where there are *n* actuators and *m* end-effector locations. The locations, $\mathbf{X}_d(x_{dm}, y_{dm}, z_{dm})$, of the end-effector of the manipulator, the needle tip, is calculated from:

$$\mathbf{X}_d = \mathbf{U}_1 + \frac{z_{dm}}{P}(\mathbf{U}_2 - \mathbf{U}_1) \tag{8}$$

where $\mathbf{U}_1(x_1, y_1, 0)$ and $\mathbf{U}_2(x_2, y_2, p)$ are the workspace of the two parallel planes, each with 2^n end-effector coordinates, (x_{im}, y_{im}, z_{im}) , in plane *i*, *p* is the parallel distance between the planes and the origin, (0,0,0), is the center point of p_1 before any perturbation. Considering the system without external forces, neglecting effects of $\mathbf{f}_{ext}$ and **W,** the position of the central point can be obtained from Eqs. (6) and (7) as:

$$U\mathbf{e}' = \frac{1}{\sum_i k_i}\sum_i k_i[(l_{oi} + \Delta_i + a_i\xi_i)\mathbf{w}_i - l_{oi}\mathbf{v}_i] \tag{9}$$

Defining a dimensionless stiffness as the ratios of stiffness springs, $\mu_i = k_i / k_1$ yields:

$$U\mathbf{e}' = \frac{1}{\sum_i \mu_i}\sum_i \mu_i[(l_{oi} + \Delta_i + a_i\xi_i)\mathbf{w}_i - l_{oi}\mathbf{v}_i] \tag{10}$$

Equation (10) shows that when there are no external forces, the output displacements of the plane actuation

are functions of the ratio of the interconnection spring constants, and not the constants themselves. Equations (8) and (10) show that the workspace of the manipulator is determined by the ratios of spring stiffness and the distance between two plane actuation modules. With the selection of these parameters, the manipulator workspace and accuracy can be optimized.

The system's ability to resist disturbance forces is measured by its effective stiffness. This stiffness at a distance from the plane of the 2nd actuator with needle compliance is:

$$K_{eq,tip} = \frac{k_{eq1}k_{eq2}p^2}{k_{eq1}(p+\xi)^2 + k_{eq2}\xi^2} \tag{11}$$

where p is the distance between the planes and ξ is a distance from p_2 towards the prostate. The variables k_{eq1} and k_{eq2} are the equivalent stiffness at connected points in the actuation modules. The equivalent stiffness in the plane actuation modules can be written as:

$$\begin{bmatrix} k_{eqx} \\ k_{eqy} \end{bmatrix} = \sum_i \begin{bmatrix} k_i |\cos\varphi_i| \\ k_i |\sin\varphi_i| \end{bmatrix} \tag{12}$$

5. Analytical Results.

Using the above manipulator analytical model and the parameters shown in Tables I and II, the predicted performance of the experimental manipulator discussed in Section VI was calculated.

Figure 7a shows the needle workspace at penetrations from 60 to 130mm. Figure 7b shows the cross section of the workspace at a penetration of 110mm. The system design produces the required workspace. Changing the stiffness of each spring while maintaining the spring ratios does not affect the workspace. Increasing the spring constants will increase the stiffness of the system. However, for a given actuator extension, the spring constants are limited by the maximum actuator forces.

In operation, the manipulator will be guided by a surgeon using real-time visual images. So the absolute position accuracy is not critical. However it is essential that the manipulator is able to reach to within +/- 5mm of any point in the prostate. As discussed above, a binary system's tolerance is determined by its configuration and the number of actuators. This system with 12 binary actuators can reach 4096 (2^{12}) points. In general, these points will not be distinct or uniformly distributed over the workspace. Here, the actuator springs are chosen to have different spring rates to eliminate system symmetries that results in nondistinct points.

To evaluate the manipulator accuracy, 1000 random targets in the workspace were chosen and the minimum distance from the closest possible end-effector position to each of these points was calculated. Figure 8 shows the distribution of these error distributions. The average distance and standard deviation, for a random point to the nearest possible end-effector point in the entire workspace are 0.68mm and 0.51mm, respectively. The same values for a prostate sized workspace are 0.41 mm and 0.21 mm. Clearly, the manipulator design meets its positional requirements (see Figure 8).

Figure 9 shows the distribution of system stiffness in the radial direction at points 110mm from the perineum. The values in the other directions perpendicular to the needle are similar. This figure shows that the stiffness of the system is quite uniform. The radial stiffness for any point in workspace is within 10% of the average stiffness of the system. It might be noted that the stiffness of the experimental system is relatively low due to the low spring rate to prevent saturation of the experimental actuators. As discussed in Section VIII the actuator forces

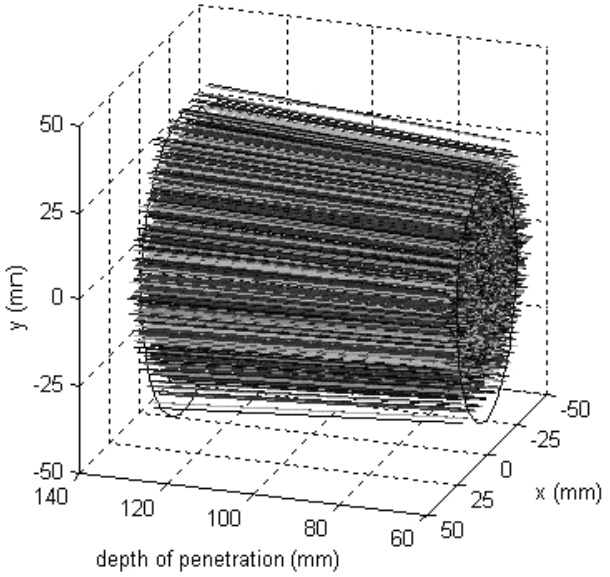

(a) Needle workspace

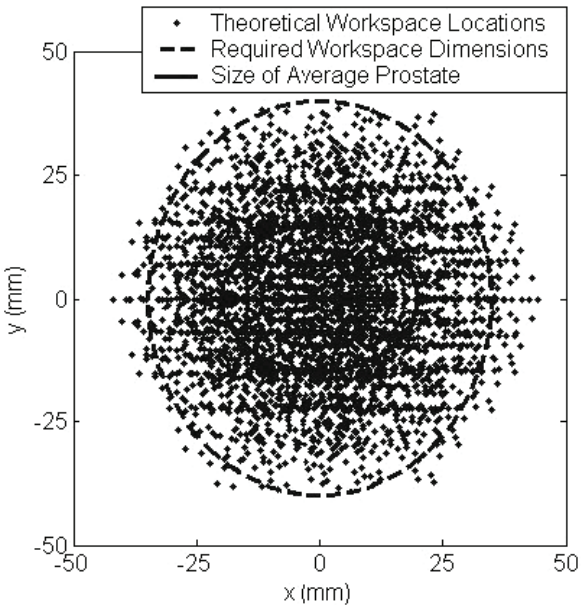

(b) Workspace at insertion depth of 110mm

Figure 7. Analytically predicted workspace of the MRI manipulator

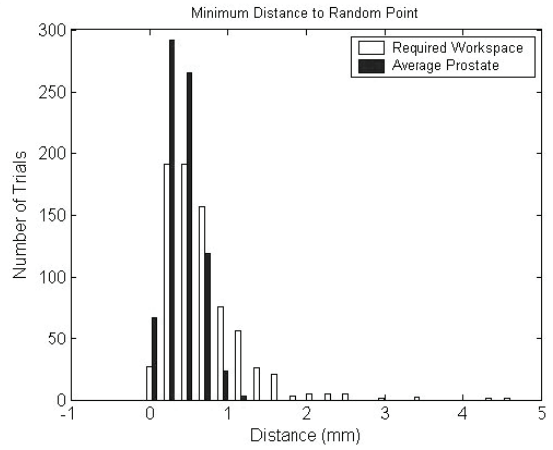

Figure 8. Minimum distances from a reachable end-effector point to randomtarget location

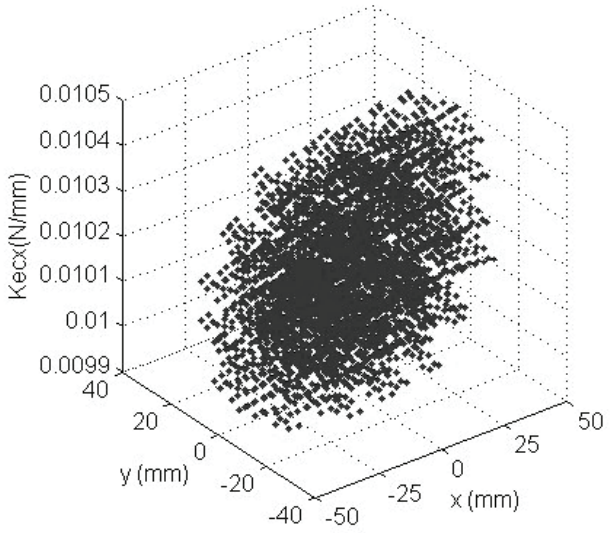

Figure 9 . Distribution of system stiffness at 110mm beyond perineum wall

are limited to current limitations of our laboratory's fabrication processes.

6. Experimental System Description

To validate the effectiveness of the MRI manipulator approach an experimental laboratory prototype of the system was fabricated and tested (see Figure 1b). This system has 12 bistable DEA actuators. These actuators have three layers of polymer material in each cone. The dimensions for each actuator plane are given in Table III. The planes are 180mm apart. To facilitate the fabrication of this laboratory prototype its size is somewhat larger than would be required for a clinical system. To measure the needle motions a three-dimensional position sensor was used in the experiments on this research [17]. This device is an electromagnetic tracker and it can measure the position and orientation (6 DOF), with RMS accuracies of 1.4 mm and 0.5°. The moving sensor has OD 1.3 mm; length 6.5 mm and 90 Hz data rate. This measuring device is widely used for the experiments for the medical instrument tracking measurements (laproscopes, endoscopes, etc.). The sensor was mounted on the needle tip (see Figure 1b).

To verify the MRI compatibility of the device it was operated in a three Tessler clinical MRI at Harvard's Brigham and Woman's Hospital [16]. These tests on the assembled system confirmed previous results on individual actuators that showed the DEA technology is MRI compatible [7,12]. Specifically, the system is not degraded by the high magnetic fields and with conventional filtering of the electrical circuits the MR image is not degraded. A complete discussion of these tests is beyond the scope of this paper [16].

The kinematic workspace of the needle was studied in the laboratory. Fifty-four random inputs were selected from 4096 possible inputs. This reduced number of inputs was selected based on time constraints (see Figure 10). The dotted ellipse shows the size of the required workspace for prostate detection and treatment. The inner green circle shows the size of average prostate. It can be seen that the size of the workspace is essentially the same as that predicted by analysis and meets the medical requirement.

The analytical results and experimental measurements are compared in Figure 11. The data has been normalized to account for differences in the positioning of the base of the experimental system. The green circle shows the size of an average prostate. In this area, the average distance between the simulated and experimental points is about 3mm, which is smaller than 5mm, the required accuracy. It should be noted that the sensor itself has an RMS error of about 1.4 mm suggesting that more precise laser measurements and calibration currently underway will significantly reduce the meaured experimental errors.

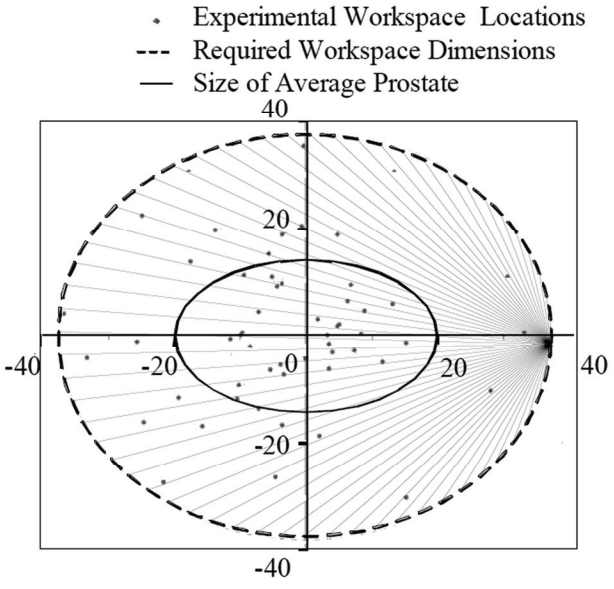

Figure 10. Needle experimental workspace

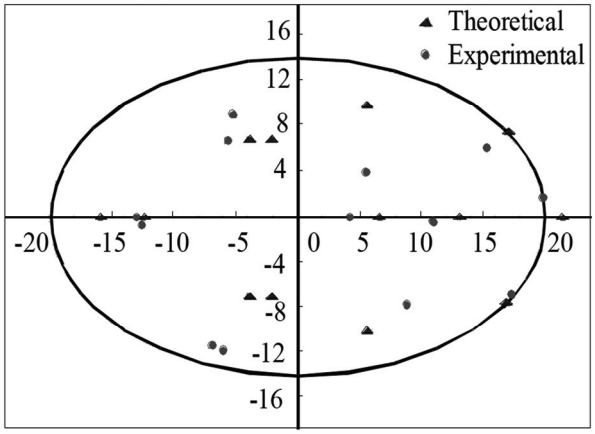

Figure 11. Needle placement performance in the prostate workspace

7. Summary and Conclusions

It is shown that a manipulator based on elastically averaged binary dielectric elastomer actuators is a promising approach to detect and treat prostrate cancer within the bore of an MRI. This manipulator precision and workspace is shown experimentally and analytically to meet the medical requirements. The stiffness of the elastic averaging actuation is lower than what would be appropriate for a clinical system to prevent actuator saturation. This however is not a fundamental limitation of the concept. It is due to the relatively small chosen number of layers of polymer used in the actuators. This choice was dictated by the time required to fabricate the systems using the simple processes available for this one-of-kind experimental system. An automated fabrication process that would eliminate this limitation is now being developed.

Other potential applications of precise robotic needle placement using MR imaging include the detection and treatment of breast cancer, endovascular surgeries, and spinal procedures are also being investigated.

8. Acknowledgements

The important contributions of Dr. Daniel Kacher, Dr. Joseph Roebuck and Dr. Simon DiMaio of Brigham and Women's Hospital (BWH) are truly appreciated.

REFERENCES

[1] Chirikjian G.S., Inverse Kinematics of Binary Manipulators Using a Continuum Model, Journal of Intelligent and Robotic Systems, Volume 19 , No. 1. May 1997, Pages: 5 – 22.

[2] Hafez, M., Lichter, M., Dubowsky, S., "Optimized Binary Modular Reconfigurable Robotic Devices," IEEE/ASME Transactions on Mechatronics, Vol. 8, no. 1, pp. 18-26, March 2003.

[3] DeVita, L.M., Plante, J.S. and Dubowsky, S., "The Design of High Precision Parallel Mechanisms using Binary Actuation and Elastic Averaging: With Application to MRI Cancer Treatment," Proceeding of the 2007 IFToMM World Congress on Machines and Mechanisms, Besançon, France, June 17-21, 2007.

[4] Sujan, V., Lichter, M., Dubowsky, S., "Lightweight Hyper-redundant Binary Elements for Planetary Exploration Robots," Proc. 2001 Int. Conf. on Advanced Intel. Mechatronics, Como, Italy, July 2001.

[5] Plante, J.,S., and Dubowsky, "Large-Scale Failure Modes of Dielectric Elastomer Actuators," The International Journal of Solids and Structures, Vol. 43, Nos. 25-26, Dec., 2006, pp 7727-7751.

[6] Plante, JS., Santer, M., Dubowsky, S., Pellegrino, S., "Compliant Bistable Dielectric Elastomer Actuators for Binary Mechatronic Systems," Proc. of the 2005 ASME Mechanism and Robotics Conference, September 2005, Long Beach, CA.

[7] DF Kacher, et al. "Development of a Reconfigurable MRI Coil using Electrostrictive Polymer Artificial Muscle Actuators," Proc of the Int. Soc. of Magnetic Resonance in Medicine, May, 2004, Kyoto,.

[8] Wingert, A., Lichter, M.D., Dubowsky, S. "On the Kinematics of Parallel Mechanisms with Bi-Stable Polymer Actuators." Proc. 8th Int. Sym. on Advances in Robot Kinematics, Barcelona, June 2002

[9] Slocum, A., Precision Machine Design, Society of Manufacturing Engineers, 1992.

[10] Y. Koseki, K. Koyachi, T. Arai, and K. Chinzei, "Remote Actuation Mechanism for MR-compatible Manipulator Using Leverage and Parallelogram -Workspace Analysis, Workspace Control, and Stiffness Evaluation", Proc. of ICRA2003, pp. 652-657, 2003

[11] . Krieger, et al "Design of a Novel MRI Compatible Manipulator for Image Guided Prostate Interventions," IEEE Trans. on Biomedical Engr., Vol. 52, No. 2, pp. 306-313, 2005

[12] Vogan, J., et al, "Manipulation in MRI Devices using Electrostrictive Polymer Actuators: With an Application to Reconfigurable Imaging Coils," Proc. IEEE ICRA, New Orleans, April 2004.

[13] DeVita, L.M., Plante, J.S. and Dubowsky, S., "The Design of High Precision Parallel Mechanisms using Binary Actuation and Elastic Averaging: With Application to MRI Cancer Treatment," Proc 2007 World Congr on Machines and Mech., Besançon, France, June, 2007.

[14] Jemal, A., et al, "Cancer Statistics, 2005," C.A.: A Cancer Journal for Clinicians, Vol. 55, pp. 10-30, 2005.

[15] Nag, S., et al, "American Brachytherapy Society (ABS) Recommendations for Transperineal Permanent Brachytherapy ofProstate Cancer," Intern. Jour. of Radiation Oncology Biology Physics, Vol. 44, No. 4, pp. 789-799, 1999.

[16] Lauren Devita "An MRI Compatible Manipulator for Prostate Cancer Detection and Treatment," MS Thesis, Massachusetts Institute of Technology, Cambridge, MA, June, 2007.

[17] A miniBIRD model 800, Product of Ascension Technology, Inc, http://www.ascension-tech.com/prducts/minibird.

